

Cosmology with the Sunyaev-Zel'dovich Effect.



Fernando Atrio-Barandela.

Física Teoría. Departamento de Física Fundamental.

Facultad de Ciencia. Universidad de Salamanca.

Collaborators: R. Génova-Santos, C. Hernández-Montegudo, A. Kashlinsky, J.P. Mückel.

Summary.

- 1.- The Sunyaev-Zeldovich Effect.
- 2.- The Missing Baryon Problem.
- 3.- Effect of the WHIM in the CMB.
- 4.- Observational Prospects.
- 5.- Measuring Bulk Flows.

The Sunyaev-Zeldovich Effect.

The Thermal/Kinematic Sunyaev-Zeldovich Effect.

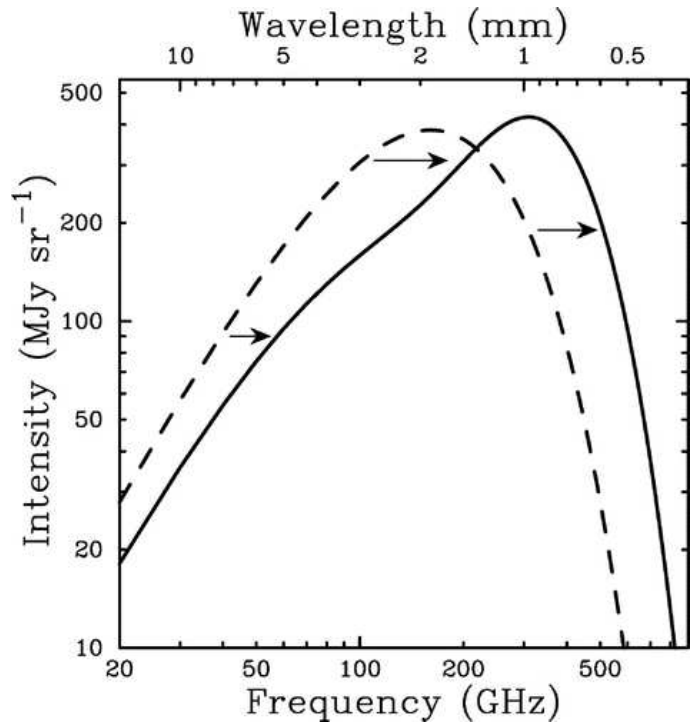
- Secondary CMB temperature anisotropy generated by the hot Intra-Cluster Medium.
- It has two components: (a) due to the thermal motion of electrons in the potential wells of clusters of galaxies (TSZ) and (b) associated to the motion of a cluster as a whole (KSZ):

$$\left(\frac{\Delta T}{T_o}\right)_{TSZ} = g(\nu)y_o \quad y_o = \frac{k_B}{m_e c^2} \sigma_T \int n_e T_X dl ; \quad \left(\frac{\Delta T}{T_o}\right)_{KSZ}(\hat{n}) = \frac{\vec{v}_{cl} \hat{n}}{c} \int n_e dl$$

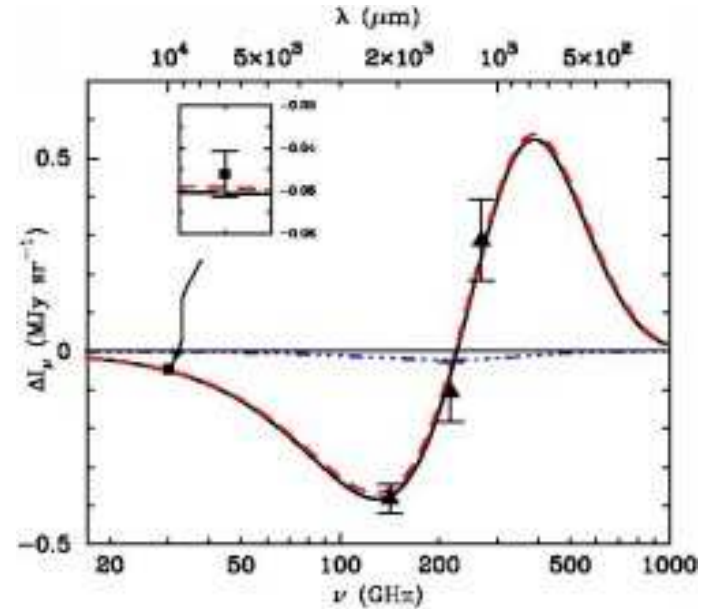
- The TSZ effect is a **distortion of the CMB spectrum** and therefore is frequency dependent:

$$g(\nu) = (x \coth(x/2) - 4) \quad x = h\nu/kT$$

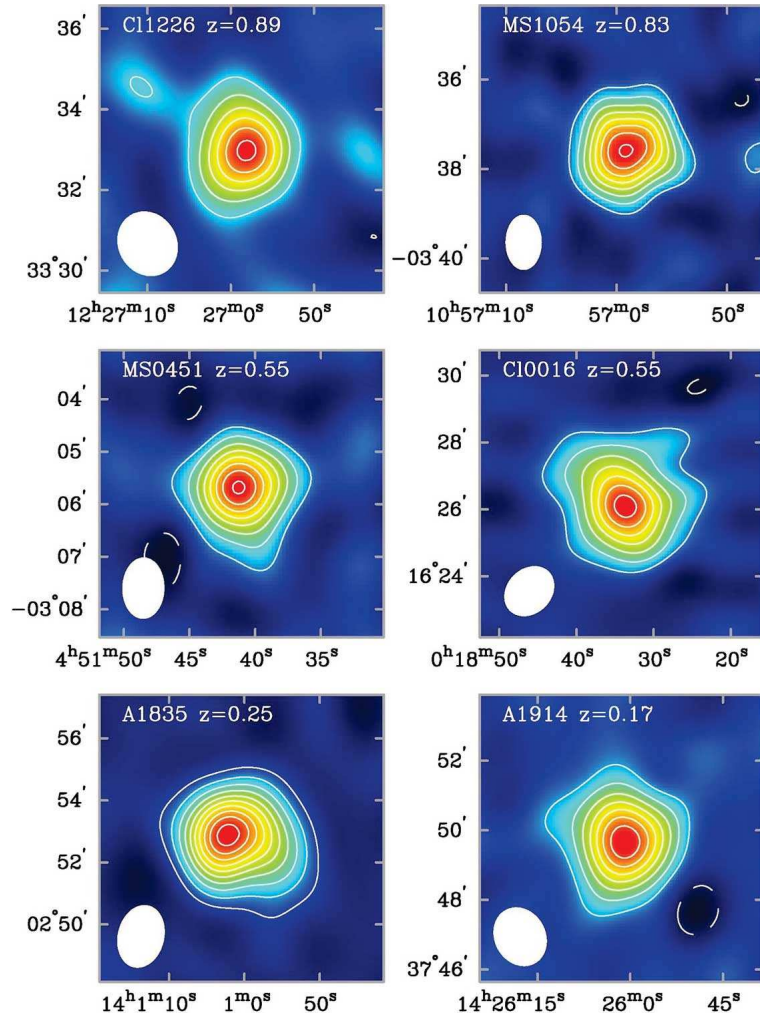
- $T_x \sim 10\text{KeV}$, $v_{cl} \simeq 300\text{km/s}$ \Rightarrow $\Delta T_{TSZ} \sim 300\mu\text{K}$, $\Delta T_{KSZ} \sim 15\mu\text{K}$



Caption: (left) spectral distortion produced by a cluster 10^3 times more massive than COMA. (From Sunyaev-Zeldovich A&SpSc 1980).



Caption: (right) intensity variation for A2163; dashed, dotted and solid lines correspond to the best fit to TSZ, KSZ and combined signals. The peculiar velocity estimated is $v_p = 410_{-850}^{+1030+460}$ km/s. (From Carlstrom et al ARAA 2003).



The TSZ effect is independent of Redshift.

Caption: Clusters with similar X-ray luminosity at different redshifts have a very different X-ray Flux, but similar TSZ signal (from Carlstrom et al ARAA 2003).

Cosmology with the SZ effect.

- ♣ Cluster counts: $\Omega_\Lambda, \sigma_8, w, w'$.
- ♣ Thermal Energy: Cluster formation and evolution.
- ♣ Non-cluster signals: Missing Baryons.
- ♣ Cluster peculiar velocities: Large Scale Velocity fields.

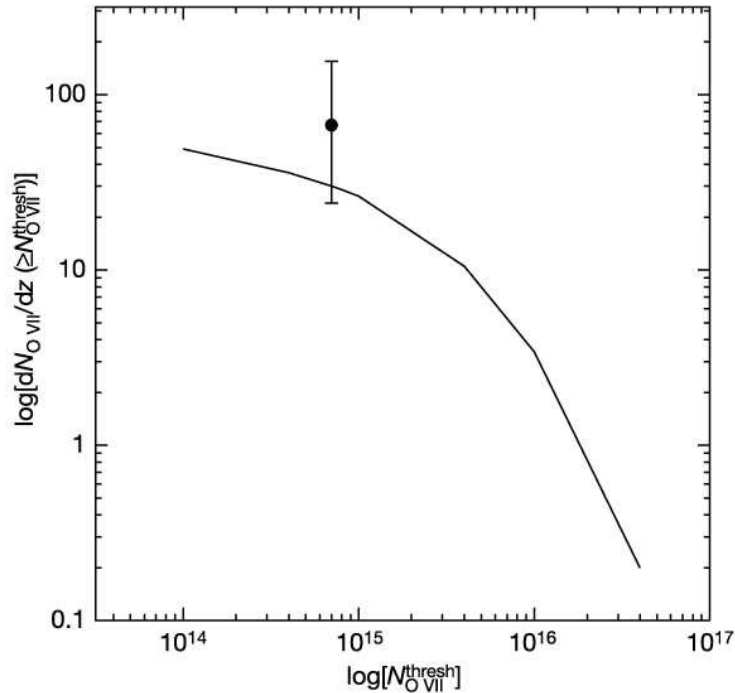
The Missing Baryon Problem.

Baryon Budget.

| | Inferred from | Ω_b (%), $h_{70} = 1$ |
|-------------------------------|---|------------------------------|
| Predicted | BBN + D/H | 4.4 ± 0.4 |
| | CMB anisotropy | 4.6 ± 0.2 |
| Observed at $z > 2$ | Ly $-\alpha$ forest | > 3.5 |
| Observed at $z < 2$ | Stars | 0.26 ± 0.08 |
| | HI + HeI + H ₂ | 0.080 ± 0.016 |
| | X $-\alpha$ ray gas in clusters | 0.21 ± 0.06 |
| | Ly $-\alpha$ forest | 1.34 ± 0.23 |
| | Warm + Warm $-\alpha$ Hot O _{VI} | $0.6^{+0.4}_{-0.3}$ |
| | Total (at $z < 2$) | $2.5^{+0.5}_{-0.4}$ |
| Missing Baryons (at $z < 2$) | TOTAL | $2.1^{+0.5}_{-0.4}$ |

From Fukugita & Peebles 2004.

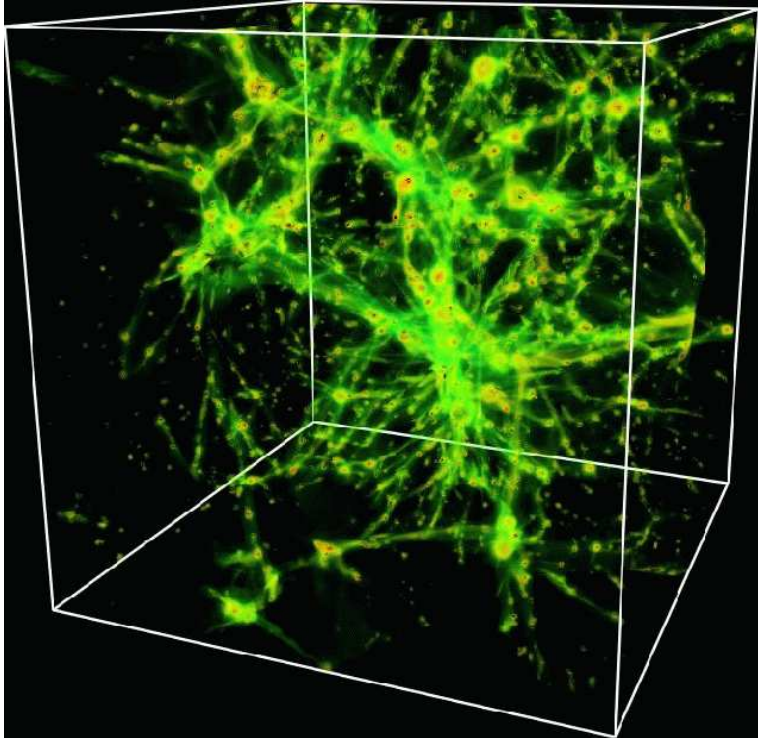
Missing Baryons in the local Universe.



- Hydrodynamical simulations predict the “cosmic web” of $10^5 - 10^7\text{K}$ should contain about half the baryons in the nearby Universe (Cen & Ostriker 1999, Davé et al 2001).
- Those structures should appear as a forest of highly ionized metal absorption lines in X-ray spectra of background sources (Hellsten 1998, Perna & Loeb 1998).
- Nicastro et al 2005 observed the X-ray forest with Chandra grating observations.

Caption: Evidence of two filaments in the line of sight of Mkn 421 at redshifts $z=0.011, 0.027$; the temperature of these systems is $\log(T/\text{K})=5.8-6.4$.

The Distribution of Baryons.



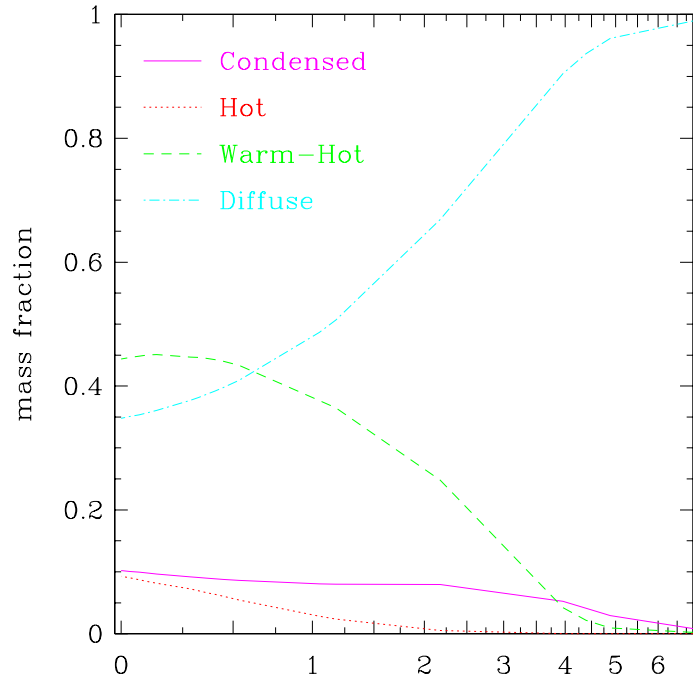
Most of the warm/hot baryons reside in diffuse large scale structures with median overdensity around 10-30, not in virialized objects such as galaxy groups or virialized dark halos (Dave et al 2001).

Caption: WHIM gas simulation at $z=0$ with temperatures $T \sim 10^5 - 10^7$ K. The gas is distributed as a "web of cosmic filaments" scales between large scale fluctuations and strongly non-linear scales within halos.

Green: $\delta > 10$

Yellow: $\delta > 100$

Red: $\delta > 1000$, sites of galaxy formation



z

Simulations indicate that baryons are distributed in 4 broad phases whose ratios change with redshift:

- Condensed: stars and cool galactic gas; $\delta > 1000$, $T < 10^5$ K.
- Hot: gas in clusters and large groups; $T > 10^7$ K.
- Warm-Hot: median overdensity $\delta \sim 10 - 30$; $T \sim 10^5 - 10^7$ K.
- Diffuse: photoionized intergalactic gas that gives rise to Ly- α absorption systems; $\delta < 1000$, $T < 10^5$ K.

Caption: Baryon fraction in the different phases as a function of redshift (from Davé et al. 2006).

Effect of the WHIM in the CMB.

Motivation.

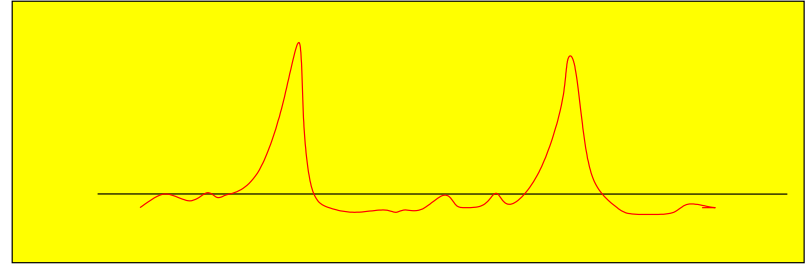
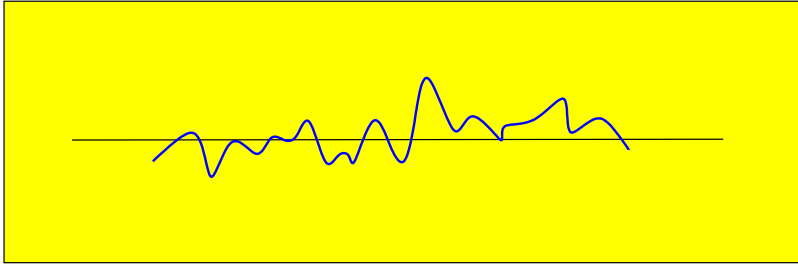
- The IGM contains a substantial fraction of all baryons in the Universe.
- The WHIM gas is not locked in collapsed objects: Filaments, outskirts of clusters of galaxies...
- 1/4 of the soft X-ray background at 0.7 KeV arises from the WHIM, 3/4 of which come from $z < 0.1$. Since

$$L_X \sim n_e^2 T_x^{1/2}, \quad \Delta T_{TSZ} \sim n_e T_x$$

Since the gas is mildly warm and diffuse, it could leave a detectable TSZ imprint on the CMB.

- The main difficulty is to give a proper description of the WHIM distribution.
- Ref: Atrio-Barandela & Mücke ApJ 2006.

The Model.

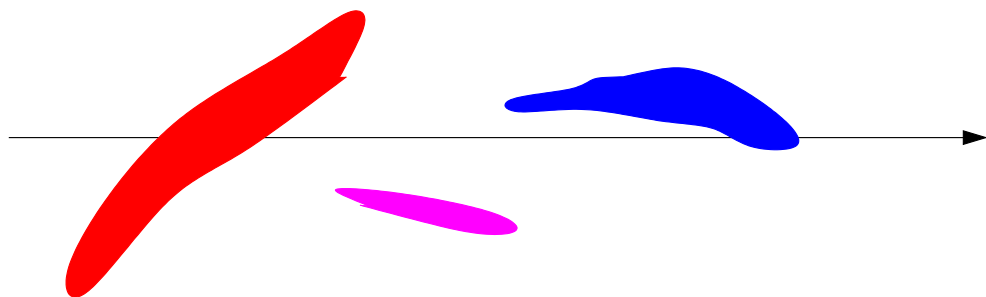


♠ (Coles & Jones MNRAS 1991): if (a) the initial density δ and velocity fields are gaussian, (b) in the non-linear regime the velocity field is gaussian and (c) the continuity equation holds, THEN:

the NON-LINEAR density field ξ follows a log-normal PDF.

$$\xi = \frac{n_B(\vec{x}, z)}{n_B(z)}, \quad P(\xi) = \frac{1}{\xi \sqrt{2\pi} \Delta_B} e^{-\frac{(\log(\xi) + \Delta_B^2/2)^2}{2\Delta_B^2}}$$

Number density of WHIM filaments



Number density of electrons at each location:

$$n_B(\mathbf{x}, z) = n_0(z) e^{\delta_B(\mathbf{x}, z) - \Delta_B^2(z)/2}$$

Variance of the Baryon density field:

$$\Delta_B^2(z) = \langle \delta_B^2(\mathbf{x}, z) \rangle = D^2(z) \int \frac{d^3k}{(2\pi)^3} \frac{P_{DM}(k)}{[1 + x_b^2(z)k^2]^2}$$

δ_B linear baryon density field, $D(z)$ growth factor, $x_b(z)$ Jeans length.

Physical Parameters.

- σ_8 : Baryons are described as a continuous distribution, with a log-normal PDF. The degree of non-linear evolution is determined by σ_8 .
- γ, T_0 : The equation of state is assumed to be polytropic:

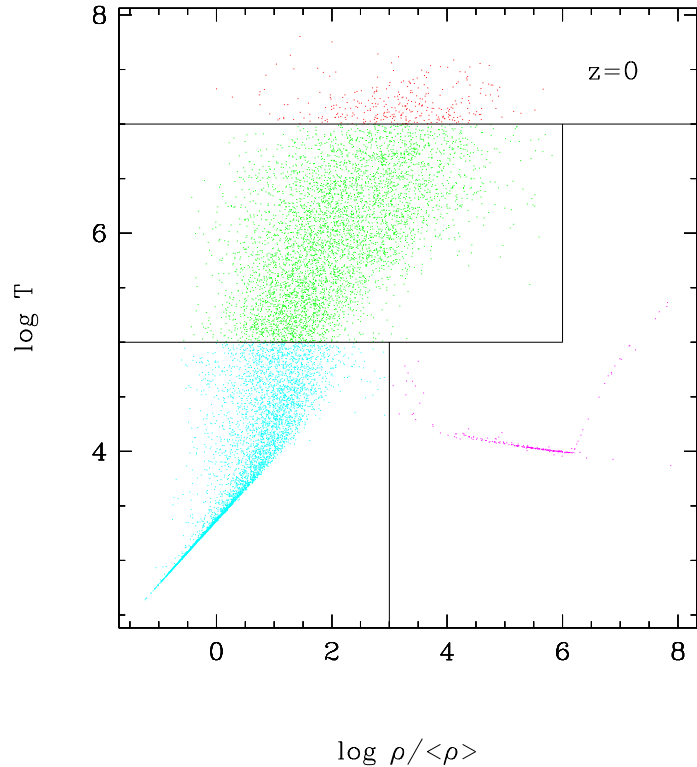
$$T(\mathbf{x}, z) = T_0(z) \left(\frac{n_B(\mathbf{x}, z)}{n_0(z)} \right)^{\gamma-1}$$

γ is the polytropic index, $T_0(z)$ temperature at mean density.

- T_m : At each redshift the Jeans length is given by the mean temperature,

$$x_b(z) = \frac{1}{H_0} \left[\frac{2\gamma k_B T_m(z)}{3\mu m_p \Omega_m (1+z)} \right]^{1/2} .$$

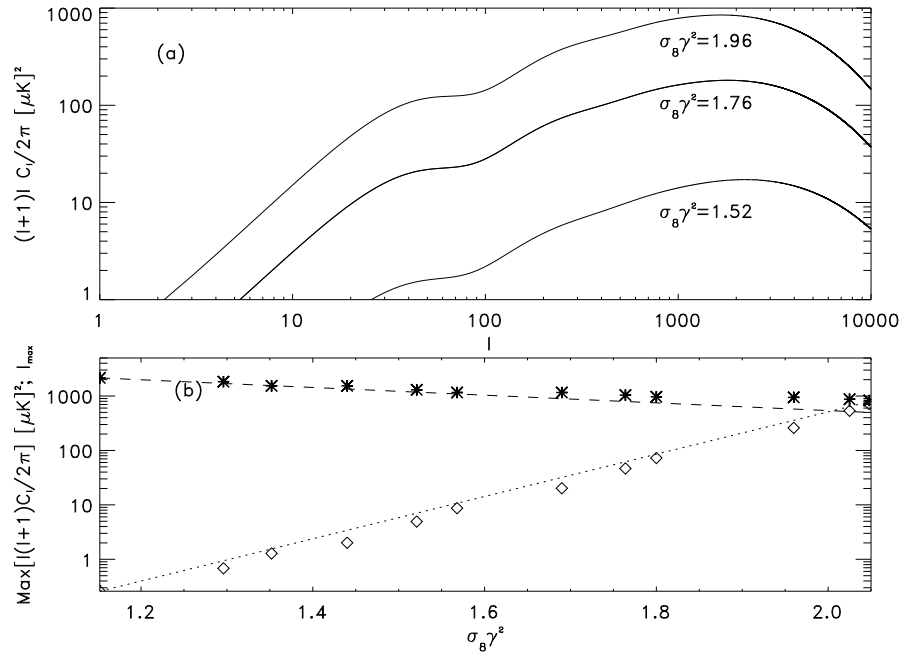
Fiducial Model.



$\gamma = 1.4$ or within (1.0,1.6);
 $T_0 = 1.4 \times 10^5 \text{K}$;
 $T_m = 1.0 \times 10^5 \text{K}$;
 $\sigma_8 = 0.8$
 $\delta < 100$
 $z_{max} = 6$

Caption: Equation of state of the gas in different phases: **condensed (violet)**, **hot (red)**, **warm-hot (green)**, **diffuse (blue)** (Davé et al 2003).

Radiation Power Spectrum.

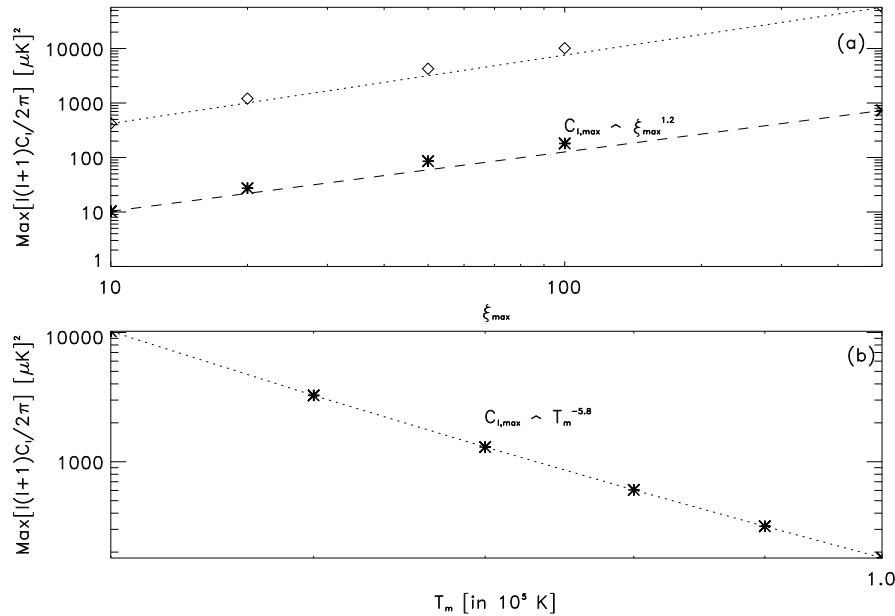


Caption: (a) CMB radiation power spectrum. The middle curve corresponds to $\gamma = 1.4$, $\sigma_8 = 0.9$.

(b) Best fit to the amplitude (dotted line) and location (dashed line) of the radiation power spectrum maxima as a function of combined gas and cosmological parameters ($\sigma_8 \gamma^2$). Asterisk and diamonds correspond to the models actually computed. The y-axis gives the maximum value in (μK^2) -diamonds- and the multipole l_{max} corresponding to the maxima -asterisks-.

Cosmological Model: $\Omega_\Lambda = 0.75$, $\Omega_{DM} = 0.21$, $\Omega_B = 0.04$, $h = 0.71$.

Scaling Relations.



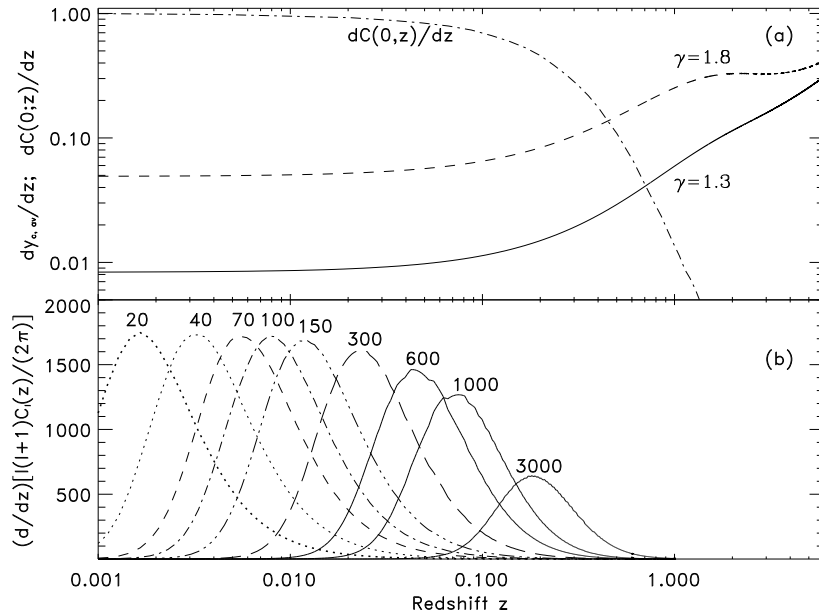
Caption: (a) Maximum amplitude as a function of maximum non-linear overdensity for two different mean temperatures: dotted line $T_m = 5 \times 10^4 \text{K}$ and dashed line $T_m = 10^5 \text{K}$.

(b) Maximum amplitude as a function of mean temperature for $\xi_{max} = 100$

$$\frac{l(l+1)C_{l,max} CL}{2\pi} \sim 430(\mu\text{K})^2 \sigma_8^7 \left(\frac{\Omega_b h^2}{0.04} \right)^2$$

$$\frac{l(l+1)C_{l,max} WHIM}{2\pi} \sim \sigma_8^{12} \gamma^{24} T_m^{-6} \xi_{max}^{1.2}$$

Differential Redshift Contribution.



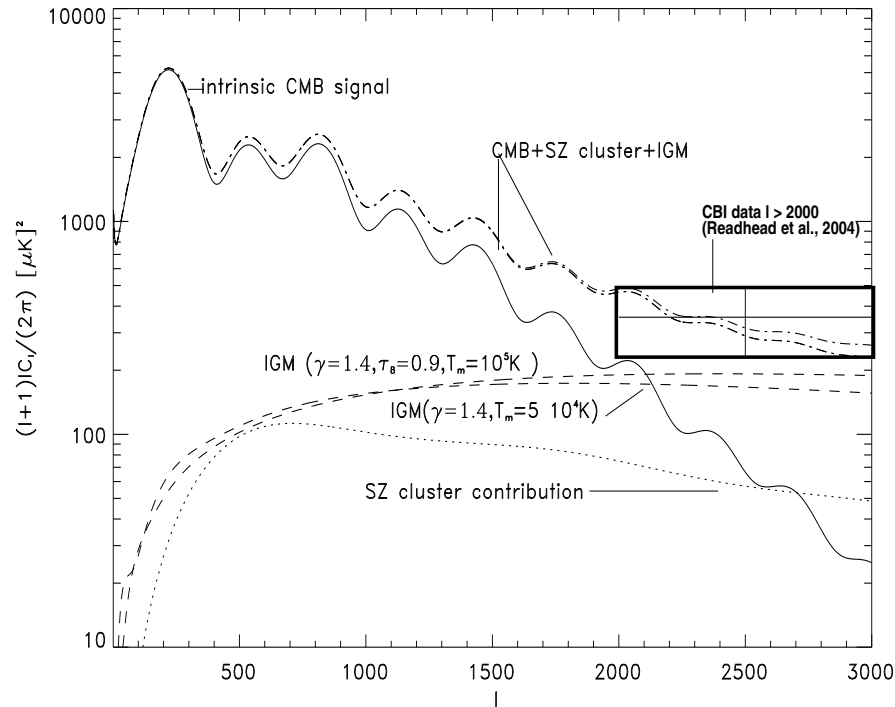
Caption: Differential redshift contribution in intervals of $\Delta z = 0.001$, $\gamma = 1.4$, $\sigma_8 = 0.9$

(a) Solid and dashed line: contribution to the spectral distortion. Dot-dashed line: contribution to the correlation function.

(b) Contribution to the radiation power spectrum for a fixed multipole.

Observational Prospects.

Indirect Evidence: CBI Power Excess at high l .



Caption: TSZ signal at 32 GHz coming from clusters (dotted line) and WHIM (dashed), intrinsic CMB (solid) and the sum of the three components (dot-dashed). Box: CBI data and 1σ error at the scales of interest.

Taken CBI as an upper limit and $\sigma_8 = 0.9$: $\gamma \leq 1.5$ at the 2σ confidence level in the redshift range [0.1-0.4].

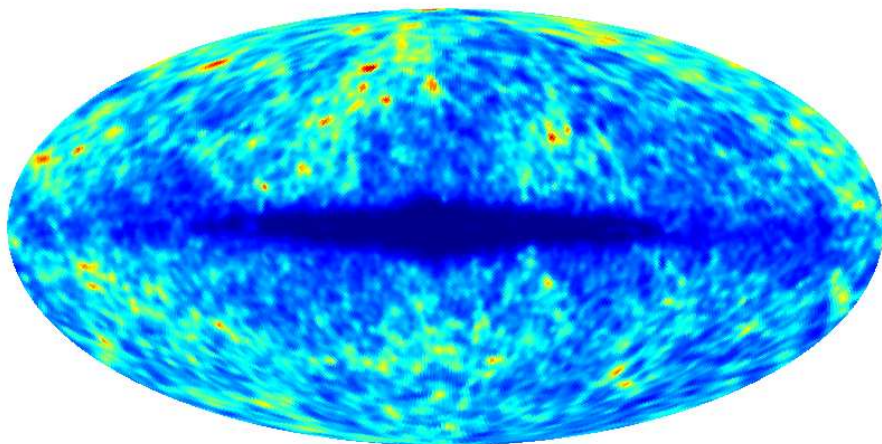
Direct Evidence.

♠ A direct detection of the WHIM contribution to CMB temperature anisotropies is made difficult because its contribution:

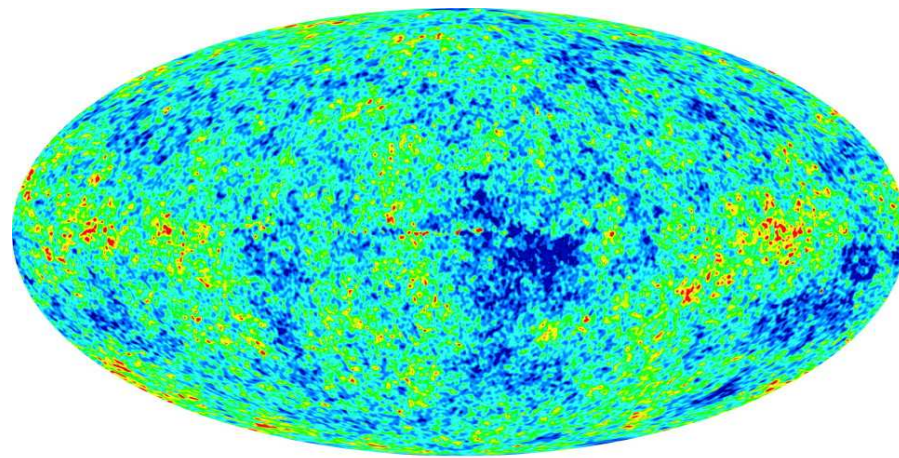
- has the same frequency dependence than the Intra-Cluster gas.
- depends strongly on ill determined model parameters.

♠ Ref: Hernández-Monteagudo et al ApJL 2004.

Galactic Templates.

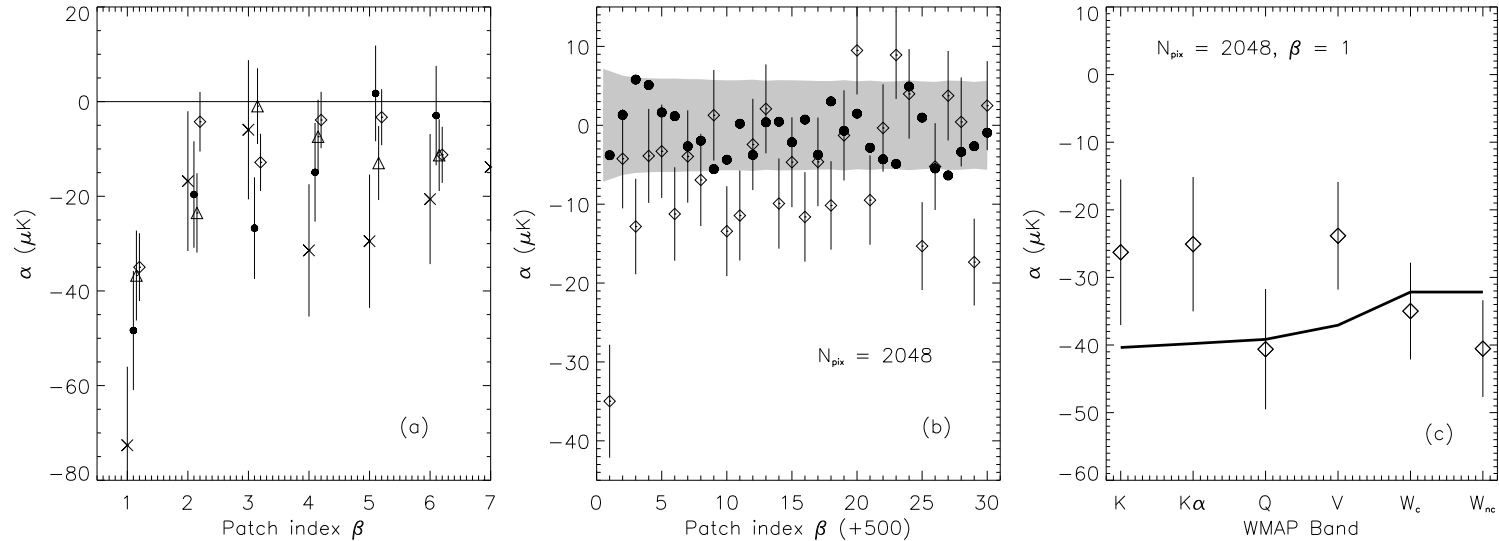


Projected density map of 2MASS galaxies

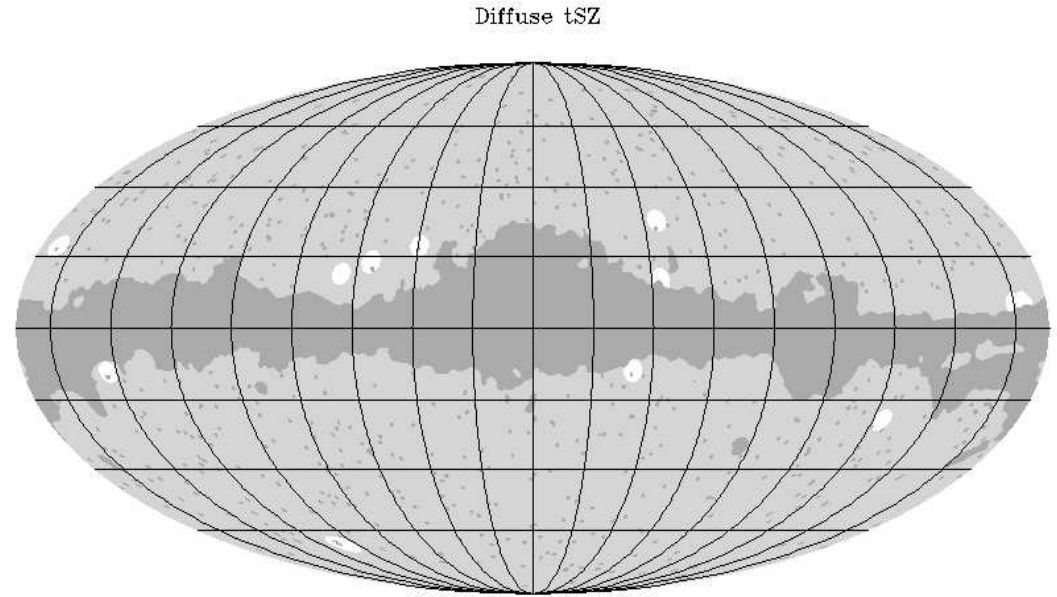
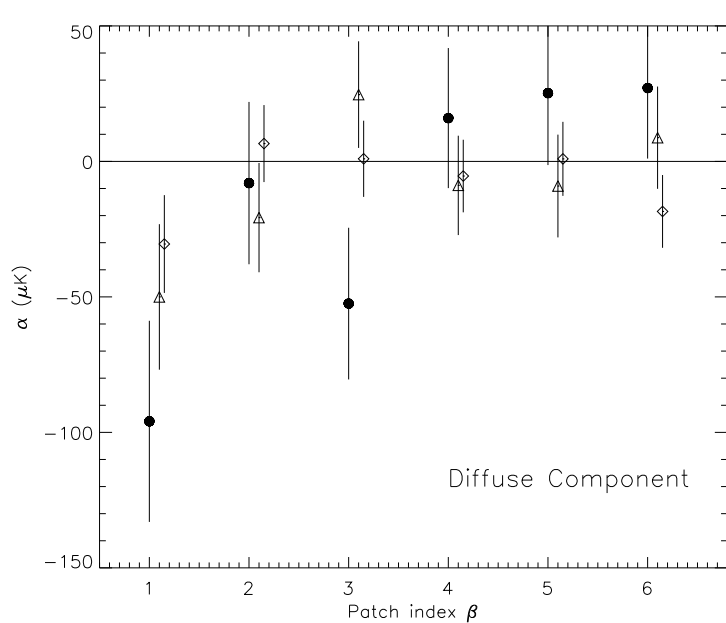


WMAP Q,V,W internal linear combination

♠ If galaxies trace the gas distribution on large scales, correlation of a template of projected galaxy density and CMB data **before and after removing the galaxy clusters** will give a direct evidence of the WHIM contribution.



Caption: (a) TSZ detection in pixel sets with the highest projected galaxy density. Crosses, filled circles, triangles and diamonds correspond to sets with 256, 512, 1024, 2048 pixels. Bars are $1 - \sigma$ errors. (b) TSZ signal for the most dense (1 to 30, diamonds) and less dense (501 to 530, filled circles) sets. Bars and band are $1 - \sigma$ errors. (c) TSZ for the different WMAP bands estimated on the densest set of 2048 pixels. The solid line represents the expected frequency dependence fitted to the cleanest bands.



Caption: Left: The TSZ signal still remains once all known clusters have been excised from the analysis. Right: White spots display the position of pixels not associated to known galaxy clusters giving rise to a TSZ signal. The dark grey area is masked out by the Kp0 mask. The graticule is $20^\circ \times 20^\circ$.

Conclusions.

- INDIRECT evidence from CBI needs further confirmation. Using CBI as an upper limit and $\sigma_8 = 0.9 \Rightarrow \gamma \leq 1.5$ at the 2σ c.l. in the redshift range [0.1-0.4].
- There is no DIRECT evidence of a TSZ signal coming from the WHIM.
- The TSZ due to the WHIM depends strongly on the model parameters:

$$\frac{l(l+1)C_{l,max} WHIM}{2\pi} \sim (\sigma_8 \gamma^2)^{12}$$

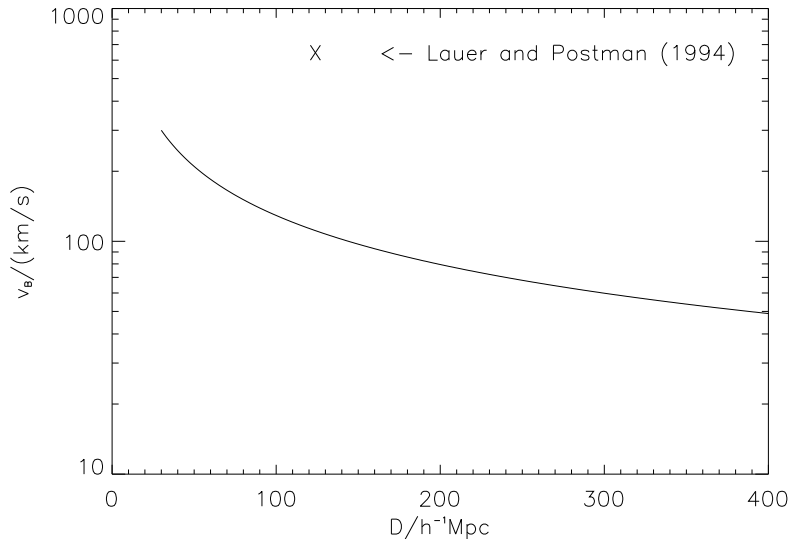
Large fractions of the total baryon content of the Universe could be stored in the WHIM without significantly altering the pattern of CMB temperature anisotropies.

Measuring Bulk Flows.

Motivation.

- Peculiar velocities of single clusters are too small to be measured: typically $10 - 30 \mu\text{K}$ for the brightest clusters, with the same frequency dependence than the CMB.
- Measurements such as A2163: $v_p = 410_{-850}^{+1030+460}$ km/s. Error bars: statistical uncertainty and systematic.
- **Peculiar velocities measurements are strong tests of alternative cosmological theories.**
- PLANCK will not improve much on individual clusters, but offers very good prospects of measuring moments of the velocity field like the **Bulk Flow** component.
- **Bulk Flow:** Average velocity of galaxies and clusters of a volume of size D .
- Ref: Kashlinsky & Atrio-Barandela ApJL 2000, Atrio-Barandela et al ApJL 2004.

Bulkflows.

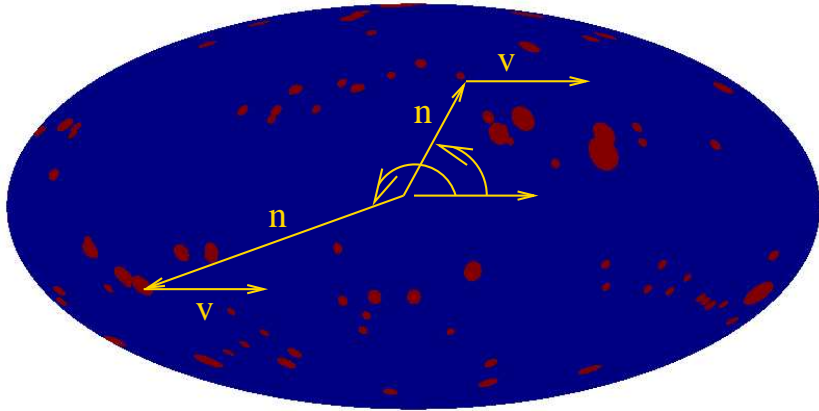


- The velocity field is coherent on large scales.
At scale D :

$$\langle V^2(D) \rangle = \frac{\Omega^{1.2}}{2\pi^2 b^2} \int P(k) W(kD) dk$$

Caption: Bulk Flow velocity amplitude for a cosmological model with parameters $\Omega_\Lambda = 0.75$, $\Omega_m = 0.25$, $h = 0.7$ $\sigma_8 = 0.8$. The data point is the Lauer & Postman (1994) measurement at $150h^{-1}\text{Mpc}$.

The Method.



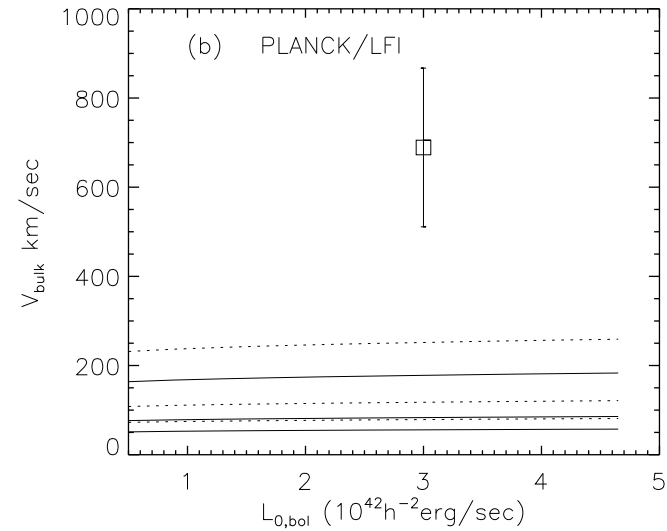
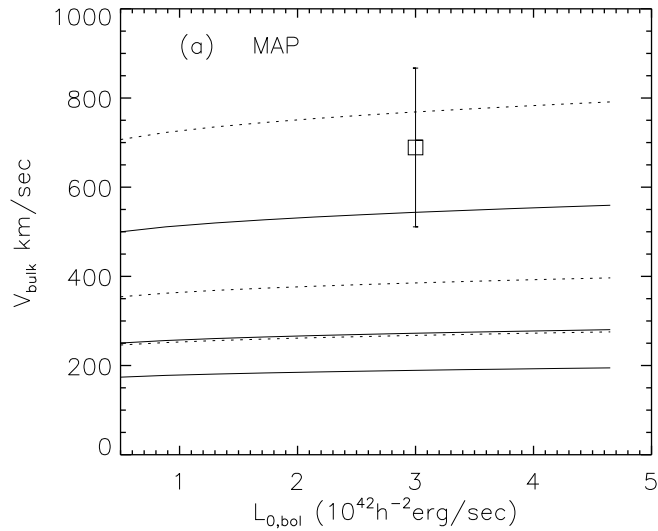
- The temperature anisotropy at cluster location is:

$$\frac{\delta T}{T_o}(\hat{n}) = \delta_{\text{TSZ}}(\hat{n})g(\nu) + \tau \frac{\vec{v}\hat{n}}{c} + \delta_{\text{CMB}}(\hat{n}) + \text{Noise}(\nu)$$

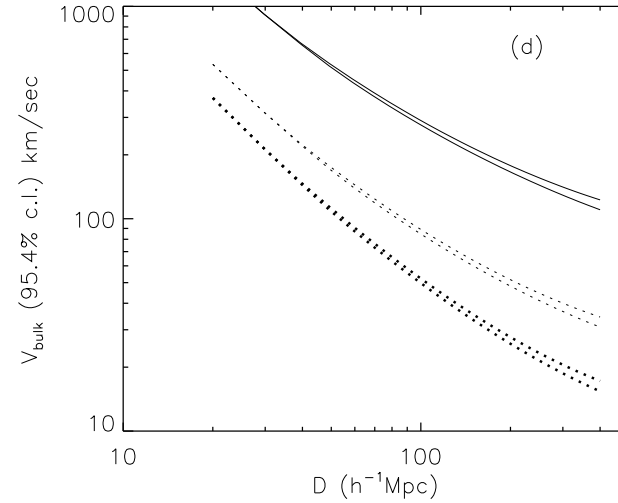
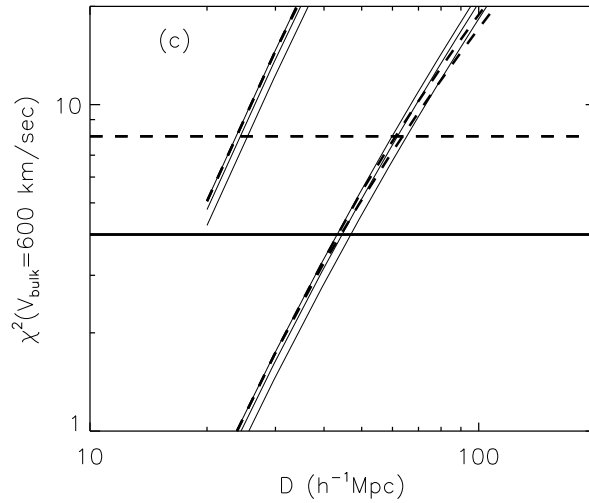
- The KSZ associated to the BULKFLOW gives rise to a dipole pattern: $\tau \frac{\vec{v}\hat{n}}{c} = \tau \frac{v}{c} \cos \theta$
- The dipole at cluster location is

$$C_{1,\nu} \simeq C_{1,\text{kin}} + C_{1,\text{th}}g^2(\nu) + \sigma_{\text{CMB}}^2/N_{\text{cluster}} + \langle (\text{Noise})^2(\nu) \rangle / N_{\text{cluster}}$$

- The main source of error is the **CMB itself**.



Caption: V_{bulk} that can be determined at 95% c.l. for volume limited catalogs. (a) WMAP, (b) PLANCK/LFI. From top to bottom, solid lines correspond to determination of the velocity amplitude at $D = 50, 100, 150h^{-1}\text{Mpc}$. Dashed lines show the measurement at the same c.l. if the three velocity component are measured. Data: Lauer & Postman (1994).



Caption: (a) From top to bottom, solid lines correspond to volume limit catalog with $L_0/L_* = (1, 2, 5) \times 10^{-3}$, dotted lines to flux-limited catalog with $F_x[0.1 - 2.4\text{KeV}] \geq (1, 2) \times 10^{-12} \text{erg/cm}^2/\text{sec}$. WMAP: lower set; PLANCK/LFI: upper set. Thick solid horizontal line corresponds to a 95% c.l measurement of the amplitude and thick dashed line, amplitude and direction. (b) Bulk flow amplitude at 95.4% c.l. vs depth of a flux-limited catalog. WMAP (solid), PLANCK/LFI (thin dotted) PLANCK/LFI+HFI (thick dotted); X-ray flux limits: $(1, 2) \times 10^{-12} \text{erg/cm}^2/\text{sec}$

Results of Simulations.

♠ For single configuration of clusters, from $z=0$ to 0.12, 100 CMB skies were generated from WMAP Q-V-W bands, TSZ signal was added, and maps were filtered **to remove the intrinsic CMB anisotropy** and the dipole was estimated.

♠ Combining the results of the three bands the error bars were:

| N_{cl} | $D/h^{-1}\text{Mpc}$ | $\sigma(D_x)/\mu\text{K}$ | $\sigma(D_y)/\mu\text{K}$ | $\sigma(D_z)/\mu\text{K}$ | $\sigma(D)/\mu\text{K}$ |
|----------|----------------------|---------------------------|---------------------------|---------------------------|-------------------------|
| 84 | 120 | 3.3 | 3.0 | 2.3 | 5.0 |
| 286 | 240 | 2.3 | 1.8 | 1.5 | 3.3 |
| 436 | 360 | 1.9 | 1.6 | 1.3 | 2.8 |

Assuming $\langle\tau\rangle = \int n_e dl \sim 10^{-3}$ then $1\mu\text{K} \sim 100\text{km/s}$, those results reproduced quite accurately the theoretical estimates.

From Simulations to Measurements.

♣ Necessary ingredient: Catalog of clusters with well known TSZ amplitude,

OR

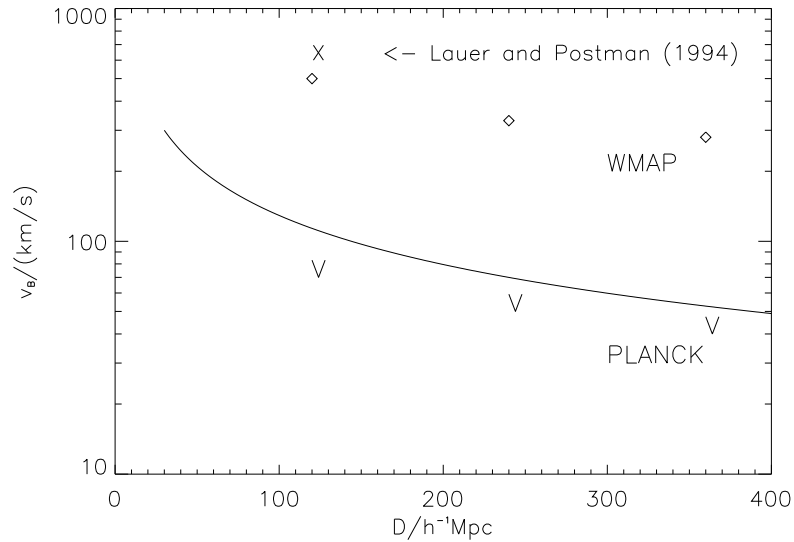
X-ray cluster catalog with well measured: cluster position, redshift (z_r), electron density (n_e), X-ray temperature (T_x), core radius (r_c, θ_c), and beta profile (β):

$$\Delta T(\theta) \sim n_e r_c \frac{\Gamma(\frac{3}{2}\beta - \frac{1}{2})}{\Gamma(\frac{3}{2}\beta)} T_x \left(1 + \frac{\theta}{\theta_c}\right)^{\frac{1}{2} - \frac{3}{2}\beta}$$

♣ Only 956 X-ray clusters are known. About 200 have all the necessary data measured.

♣ PLANCK will obtain 3,000-10,000 clusters and the measurement will be possible.

WMAP vs PLANCK.



Caption: Expected sensitivity of WMAP compared with PLANCK over the same cluster catalog: diamonds and V's give the expected 1σ error bars for WMAP and PLANCK. Solid line is the expected result for WMAP 3yr 'concordance model'.

Conclusions.

- Bulk flow measurements are an independent test of the 'gravitational instability' paradigm and the standard cosmological model.
- With the current known clusters, WMAP will set only upper limits to the bulk flow amplitude at different scales, but ...

**PLANCK will have larger frequency coverage, larger resolution,
and it will be sensitive to 70, 50 and 40 km/s at scales of 120, 240 and $360h^{-1}$ Mpc.**

and even better with PLANCK detected clusters.